

Cell tracking for live-cell microscopy using an activity-prioritized assignment strategy

Karina Ruzaeva
AICES Graduate School
RWTH Aachen
Aachen, Germany
IBG-1: Biotechnology
Forschungszentrum Jülich GmbH
Jülich, Germany
ruzaeva@ices.rwth-aachen.de

Jan-Christopher Cohrs
AICES Graduate School
RWTH Aachen
Aachen, Germany
cohrc@ices.rwth-aachen.de

Keitaro Kasahara
IBG-1: Biotechnology
Forschungszentrum Jülich GmbH
Jülich, Germany
kasahara@fz-juelich.de

Dietrich Kohlheyer
IBG-1: Biotechnology
Forschungszentrum Jülich GmbH
Jülich, Germany
d.kohlheyer@fz-juelich.de

Katharina Nöh
IBG-1: Biotechnology
Forschungszentrum Jülich GmbH
Jülich, Germany
k.noeh@fz-juelich.de

Benjamin Berkels
AICES Graduate School
RWTH Aachen
Aachen, Germany
berkels@ices.rwth-aachen.de

Abstract—Cell tracking is an essential tool in live-cell imaging to determine single-cell features, such as division patterns or elongation rates. Unlike in common multiple object tracking, in microbial live-cell experiments cells are growing, moving, and dividing over time, to form cell colonies that are densely packed in mono-layer structures. With increasing cell numbers, following the precise cell-cell associations correctly over many generations becomes more and more challenging, due to the massively increasing number of possible associations.

To tackle this challenge, we propose a fast parameter-free cell tracking approach, which consists of activity-prioritized nearest neighbor assignment of growing cells and a combinatorial solver that assigns splitting mother cells to their daughters. As input for the tracking, Omnipose is utilized for instance segmentation. Unlike conventional nearest-neighbor-based tracking approaches, the assignment steps of our proposed method are based on a Gaussian activity-based metric, predicting the cell-specific migration probability, thereby limiting the number of erroneous assignments. In addition to being a building block for cell tracking, the proposed activity map is a standalone tracking-free metric for indicating cell activity. Finally, we perform a quantitative analysis of the tracking accuracy for different frame rates, to inform life scientists about a suitable (in terms of tracking performance) choice of the frame rate for their cultivation experiments, when cell tracks are the desired key outcome.

Index Terms—Cell tracking, cell activity

I. INTRODUCTION

Live-cell (time-lapse) microscopy combined with microfluidic lab-on-chip technology enables observing single-cell features, such as cell length distributions and elongation rates,

This work was performed as part of the Helmholtz School for Data Science in Life, Earth and Energy (HDS-LEE) and received funding from the Helmholtz Association and Deutsche Forschungsgemeinschaft (DFG, German Research Foundation) 333849990/GRK2379 (IRTG Modern Inverse Problems) .

with spatio-temporal resolution in 2D [1]. Unlike standard tracking tasks (i.e., high-frame rate people or car tracking), tracking living microorganisms has specific, biology-related challenges. However, considering the height of the cultivation chamber (about the size of the cell's width), cell occlusions are prevented, while in standard tracking tasks, e.g., tracking of people, objects occlusions are almost inevitable.

Generally, at the beginning of a live-cell image sequence, only few cells are present and those are sparsely distributed. In this situation, tracking, i.e., linking cells over frames including the detection of division events, is relatively straightforward. As the experiment progresses, it becomes more and more challenging to detect the correct associations, in particular in exponential growth regimes. In crowded cell colonies, with large numbers of divisions, which often cause immense and random cell displacements between consecutive frames, identifying cell associations correctly, becomes hard even for experts [2].

Compared to standard object tracking tasks with a high frame rate, where the object positions can be predicted quite accurately because of relatively small frame-to-frame object displacements [3], in microbial live-cell imaging, researchers have to deal with notoriously low frame-rates, relative to the cell doubling times. The low frame rate in such time series generally cannot be increased since illumination from live-cell imaging, when coupled with fluorescence, leads to phototoxic effects that may change the cells' growth behavior, thereby entailing the risk to distort the interpretation of the results. Consequently, without prior information on the expected division timing and splitting behavior of the cells, the inevitably low frame rates together with chaotic cell movements are leaving us dealing with many daughter cells that need to be

linked to their mothers.

To overcome these challenges, we propose a fast parameter-free tracking approach that uses ML-based segmentation as input. The tracking is based on activity-prioritized adaptive nearest neighbor linking and a combinatorial mother-daughters assignment solver, with only one term in the linking loss function. This combinatorial assignment solver uses the biologically motivated constraint that one mother is assigned to (at most) two daughters, provided that the frame rate is higher than the division rate.

A. Related work

In the literature, cell tracking methods are split into unsupervised methods, such as tracking by model evolution and tracking by detection; and supervised, usually ML-based, approaches.

In tracking by model evolution approaches, an initial segmentation is propagated over time, meaning that the result from the previous frame becomes an initialization for the next one, thereby performing simultaneous segmentation and tracking. These methods require a considerable overlap between the initialized contour and an object to be segmented, which may not be the case in the low-frame rate datasets. Besides, taking into account the variational nature of these methods, they may be computationally expensive for large cell colonies [4]–[6], making the algorithms slow compared to tracking by detection algorithms.

Tracking by detection methods split the task into detection, often in form of instance segmentation, and tracking. The segmentation is performed with a variety of available cell segmentation methods [7]–[9]. These tracking methods link the segmented cells between consecutive frames based on their similarities, i.e., by finding correspondences between cell features in successive frames. Here, cell association becomes complicated when the feature similarity of a cell to its within-frame neighbors is comparable to the similarity of the same cell in consecutive frames. Most traditional cell tracking association strategies are performed by comparing the feature vectors, where the dominant feature typically is the cell location, i.e., so-called nearest neighbor tracking [10]. In addition to the cell location, other features are utilized, e.g., spectral features of single-cell image crops [11].

Tracking by detection is performed by linking segmentation masks over time based on a loss, i.e., the “linking” measure. A simple loss is the Euclidean distance between the positions of the cell centroids. To prevent non-physiological long-distance associations, a maximal distance limit is often applied to the distances [12]. Other linking measures are based on hand-crafted features, such as morphology and features of the cell’s neighborhood [13]–[15]. The loss, which consists of several terms, requires the proper, manually tuned weighting of the loss components. That makes the algorithm hard to generalize across microorganisms featuring different growth behaviors. Besides, the cell daughters may lose the mother’s features, such as the orientation angle, after the division, making the assignment problems less trivial.

As an alternative to the feature-vector comparison, some methods utilize cross-correlation [16]. The cross-correlation-based linking shows promising results for cells with more complex morphology, but the approach is not optimized for cases, where cells look very much alike, e.g. coccoid or rod-shaped microorganisms.

To account for possible erroneous associations and segmentation imperfections, to improve the obtained cell lineage, some works propose to combine the global linking with segmentation refinement [16], [17]. But indeed, and with current improvements in the segmentation tools, the refinement may be counter-productive (shown in the Results) and even become a source of errors. Rather than aiming at deriving a single lineage, Uncertainty-Aware Tracking relies on a Bayesian approach and keeps track of all possible lineages, ranking them by their probability, shows promising results for low-frame rate datasets [2]. However, the approach is computationally expensive, extremely space demanding, and, thus, unsuitable for the analysis of big cultivation datasets, like [18].

Unsupervised cell tracking approaches are still dominant in the cell tracking field. Although, supervised ML-based cell tracking approaches exist, e.g., [19], [20]. These methods require training data, and considering every microfluidic experiment’s uniqueness (different microorganisms, microscopy setup, etc.), training and benchmark datasets are rare, and manual tracking annotations are extraordinarily laborious to produce.

II. TARGET MICROORGANISMS AND CULTIVATION DETAILS

To assess the performance of the method, the tool is tested with in-house generated test dataset of two widely used microbacteria *Corynebacterium glutamicum* (*C. glutamicum*) and *Escherichia coli* (*E. coli*).

a) *E. coli*: In biotechnology, the gram-negative bacterium *E. coli* is a well-studied model organism and an expression host for large-scale production of proteins [21]. The bacterium is rod-shaped, and about 1 μm to 2 μm long and 0.5 μm wide. *E. coli* divides uniformly, “diffusively” elongating along the cell main axis and with a cell division occurring in the middle [1]. To test our approach, the wild type strain *E. coli* MG1655 was used. The strain was cultured under anaerobic conditions in a microfluidic device for microbial single-cell analysis, coupled with time-lapse microscopy. Experiments were carried out using an inverted time-lapse live cell microscope equipped with a 100 \times oil immersion objective and a temperature incubator. Phase contrast images of the growing microcolonies were captured every five minutes. The observed average single-cell division time is 78 ± 24 min (average time between a cell’s birth and its division, calculated from the ground truth lineages). For further cultivation details, we refer to [22].

b) *C. glutamicum*: *C. glutamicum* is a gram-positive microorganism, used in industrial biotechnology for the production of amino acids, especially L-glutamate and L-lysine [23]. As *E. coli*, *C. glutamicum* has a rod-shaped cell geometry, and typical strains range from cell lengths of 2 μm to 5 μm ,

while the width is about $1\ \mu\text{m}$ [1]. In contrast to the symmetric cell division behavior of *E. coli*, *C. glutamicum* shows apical growth (i.e., the cell wall is expanding at the cell poles), and tends to divide asymmetrically into two unequal daughters. In addition, the peculiar dynamic “V-snapping” of *C. glutamicum* cells after division (Fig. 1) [24], complicates the tracking task, especially when it comes to finding correspondences between consecutive frames, when the majority of cells in a population are dividing at the same time, pushing the cells in their neighborhood. In our numerical experiments, the wild type strain *C. glutamicum* ATCC 13032 was used. The imaging parameters of the experiment are similar to the *E. coli* cultivation experiment. However, unlike in the *E. coli* experiment, phase contrast images here were captured every two minutes. The observed average single-cell division time is 79 ± 13 min. For further cultivation details, we refer to [25].

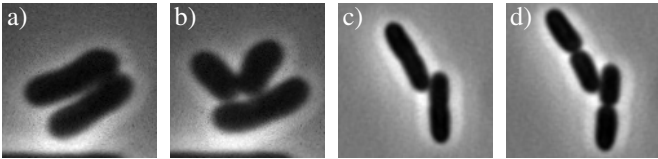


Fig. 1. Illustration of *C. glutamicum* (a-b) and *E. coli* (c-d) division events.

III. METHODS

We propose a new nearest neighbor tracking approach, which includes an “activity”-based prioritization and loss function measure, and a combination of a minimal loss single-assignment problem with Jonker-Volgenant [26] linear assignment strategy. The proposed method is efficient and robust, does not require any parameter tuning, and generalizes to many microorganisms, especially to those with low to none motility.

A. Segmentation and preprocessing

As segmentation framework, we use the recent U-net-based tool Omnipose [7]. The Omnipose network was trained on similarly looking phase contrast images of bacteria and addresses our segmentation problem well. We use the default weights and the `bact_omni` model type. We did not observe any false negative segmentation instances. The few false positives segmentation instances were filtered out by setting a known minimal cell area limit, specific to the microorganism.

B. Activity map

We propose a novel measure for cell activity that we call “activity map” (AM), highlighting the objects/cells that are likely to experience translation, division, or tilting.

The activity of cells is typically derived from tracking results. However, the approximate estimation of the cell activity, as will be shown, is possible without tracking information and may even enhance the tracking. The proposed metric is based on the intensity differences of consecutive frames combined with the cells’ segmentation masks, obtained in the segmentation step. The calculation of intensity difference of two consecutive frames was utilized by [15] as a preliminary

step for the cell tracking to estimate the cells’ motion vectors, but limited to high frame rate (less than five minutes) datasets.

To compute the proposed AM, we first calculate the moving pixel-wise standard deviation (S) over a stack of frames, i.e.,

$$S_t = \sqrt{\frac{1}{n_- + n_+ + 1} \sum_{s=t-n_-}^{t+n_+} (I_s - \overline{I_{t-n_-}, \dots, I_{t+n_+}})^2}, \quad (1)$$

where $n_-, n_+ \in \mathbb{N}$, I_s for $s \in \{1, \dots, N\}$ is the s -th image (frame) in the image stack, N is the total number of frames, and $\overline{I_{t-n_-}, \dots, I_{t+n_+}}$ denotes the average of the image stack over frames I_{t-n_-} to I_{t+n_+} . For the border regions, the interval is taken from $\max(t-n_-, 1)$ to $\min(t+n_+, N)$. The window for the calculation is specified by the user and can be tailored for the application. For general purpose visualization, we suggest taking the symmetric window ($n_- = n_+$) from t_{t-n_-} to t_{t+n_+} for $n_- < t < N - n_+$.

To calculate $a_{t,i}$, the activity of i -th cell at time t , we integrate the obtained map S_t over the corresponding segmentation mask. To reduce the influence of the cell area, i.e., bigger cells would have more activity, the value was normalized by dividing by the area, i.e.,

$$a_{t,i} = \frac{\sum_{x=0, y=0}^{X, Y} M_{t,i}(x, y) S_t(x, y)}{\sum_{x=0, y=0}^{X, Y} M_{t,i}(x, y)} \quad (2)$$

where $M_{t,i}$ is the binary segmentation mask for the i -th segmentation instance of the t -th frame, cf. III-A. As a prioritization and activity metric for cell tracking, we consider only two ($n_- = 0, n_+ = 1$) consecutive frames. The proposed activity map is illustrated in Fig. 2, where each cell’s segmentation mask was “colored” with the respective activity value.

The proposed map may be beneficial to support manual tracking annotation, attracting the analyst’s attention to the active (splitting, growing, or migrating) cells. Moreover, the AM allows automatic and straightforward “nearest neighbor” assignments for those cells that do not show any activity.

One additional use of the activity map, that we don’t explore here, is as an indicator to refine under-segmentation in the “non-active” regions by adding the “missed” non-active cell mask from the previous or the next frame. Moreover, the AM can be used to refine the over-segmentation, e.g., segmenting pieces of the chip structure or air bubbles as cells, by concluding those objects that do not move during the entire cultivation time are unlikely cells.

Additionally, by being efficient and robust, the proposed AM may be useful to adjust the cultivation conditions in real time, e.g., by indicating starving cell sub-colonies due to the lack of nutrition or other reasons.

C. Gaussian activity-based heatmap as a linking measure

Our target microorganism *C. glutamicum* is non-motile. Therefore, movement of a cell is expected only in the case of its own division or the division of the cells in its neighborhood. Moreover, the direction of the V-snap is hard or impossible

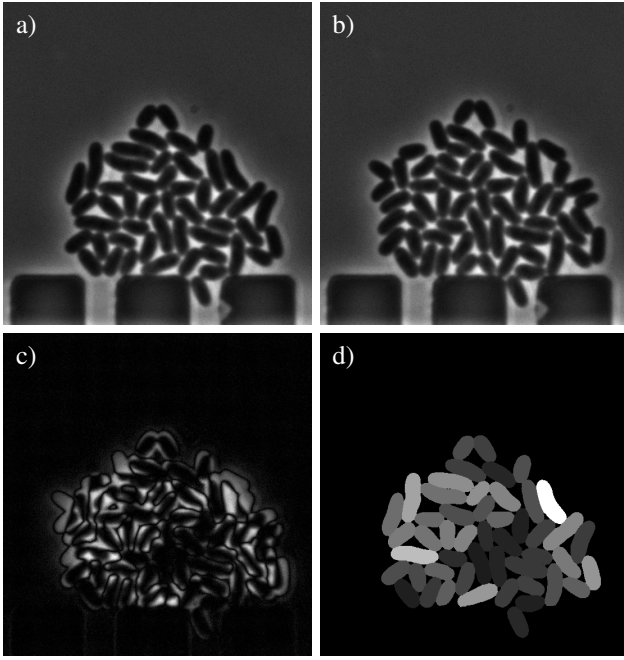


Fig. 2. Two consecutive phase contrast images I_t, I_{t+1} of *C. glutamicum* (a-b), the corresponding standard deviation S_t (c), and the activity map (d).

to predict. Therefore, a linking measure to account for the mentioned facts is desired.

As a linking measure, the traditionally used Euclidean distance between cells’ centers requires a globally set threshold to prevent non-physiological long-distance cell associations, and does not consider that some cells are less likely to divide than others. To account for these characteristics, we propose a new linking measure, a new activity-based metric that restricts the daughter’s search based on the mother’s activity and, thus, offers fewer possible candidates compared to the Euclidean distance.

As an ingredient for the linking of the cells from t to $t+1$, for each cell from t , we use a 2D Gaussian function G centered at the center of mass of the i -th cell (c_i) and width $\sigma_i > 0$:

$$G_i(x, y) = \exp\left(-\frac{1}{2\sigma_i^2}((x - c_{x,i})^2 + (y - c_{y,i})^2)\right). \quad (3)$$

Here, σ_i is proportional to the activity of the i -th cell (a_i), i.e., $\sigma_i = a_i/k$, with a scaling parameter k . Since G is strictly positive, but decaying exponentially, we reduce the number of possible candidates by treating G below 0.01 as zero. Unlike Euclidean distance thresholding, the proposed threshold is invariant to the spatial image resolution and does not need to be tuned. Fig. 3 illustrates the behavior of G with two cells similar in size, but different in activity with $k = 2.5$. This value of k is used throughout this work.

D. Prioritization-based single assignment

We propose to split the assignment in two stages: A prioritization-based single assignment of growing cells, followed by a combinatorial linear assignment of splitting cells and their daughters. The proposed assignment strategy is

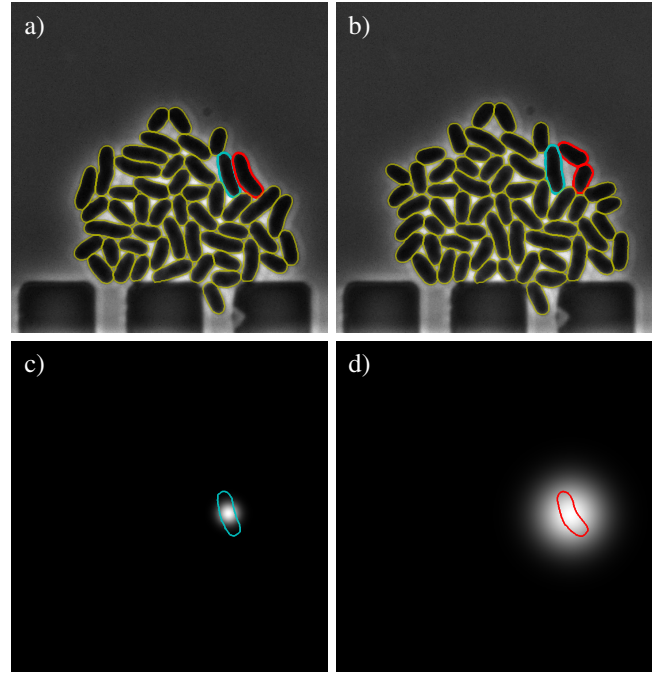


Fig. 3. Frames at times t (a) and $t+1$ (b) with highlighted cells: blue and red with relatively low and high activity in t (see Fig. 2) respectively. (b) shows the correct $t - t + 1$ assignment of the highlighted cells. (c) and (d) show the activity-based Gaussian maps G or the respective cells-the linking measure of our proposed method. Note, that (c) and (d) were computed before the assignment and without using the tracking results shown in (b).

illustrated in Figure 4. Before the assignment, we form two lists: the list of cells in frame t and frame $t+1$, where the cells in t are sorted in ascending order by activity (a_i). We formulate the linking loss between the i -th cell of frame t and the j -th cell of frame $t+1$ as follows:

$$L(i, j) = -G_i(c_{x,j}, c_{y,j}). \quad (4)$$

Here, G_i is the Gaussian map for the i -th cell of frame t , cf. Eq. 3, and $(c_{x,j}, c_{y,j}) \in \mathbb{R}^2$ is the center of mass of the j -th cell of frame $t+1$.

We pair the cells (iterating over the mothers in the sorted order) with the minimal linking loss, and check if the criterion is satisfied. As a criterion for a “valid” link, we assume that cells are not shrinking in size, i.e., a cell from frame $t+1$ has to have at least as large area as its link from frame t . If the cell shrinking over time may be expected (e.g., under famine conditions), the criterion can be tailored, according to the specific behavior of the microorganism. If the criterion is satisfied, we remove the assigned cell from the list of possible candidates of frame t and the list of frame $t+1$. After this initial assignment set, only the cells from frame t that either split (in most cases) or would have been erroneously assigned to smaller cells and their possible daughters/growing “copies”, are left without assignment. These unassigned cells participate in a double linear assignment step.

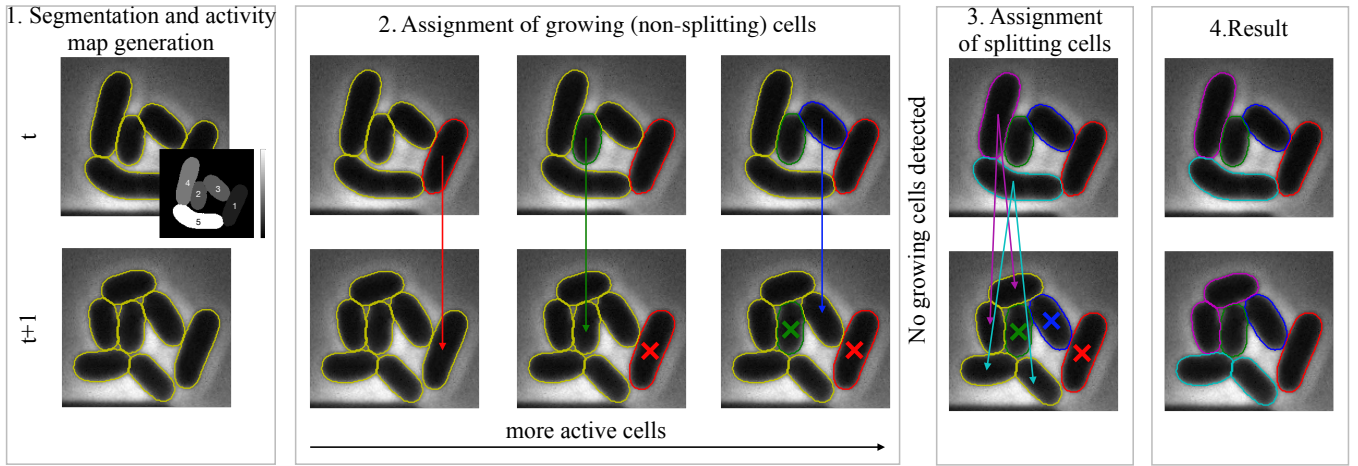


Fig. 4. The proposed tracking pipeline, which includes multi-object segmentation and activity map generation (1) and the two-step assignment strategy (2 and 3), for cells from two consecutive frames. The assignment of growing cells starts with the cell with the lowest activity (2). Once all growing cells are assigned, the remaining cells from time t and time $t + 1$ participate in the combinatorial assignment (3).

E. Linear assignment

The linear sum assignment problem is known as minimum weight matching in bipartite graphs [27]. A problem instance is described by a matrix C , where each matrix entry $C[i, j]$ is the cost (loss) of matching vertex i of the first set (a “worker”, “mother” in our case) and vertex j of the second set (a “job” or “daughter” in our case). The goal is to find a complete assignment of workers to jobs of minimal cost, i.e.,

$$\min_{X \in \mathcal{X}} \sum_i \sum_j C(i, j) X(i, j). \quad (5)$$

Here, \mathcal{X} is the set of boolean matrices X with $\min(\text{num rows}(C), \text{num cols}(C))$ non-zero entries whose rows and columns sum to at most one and where, $X(i, j) = 1$ if cell i is assigned to cell j , and $X(i, j) = 0$ otherwise.

In case of C being square, each row is assigned to exactly one column, and each column to exactly one row. Taking into account that one mother has exactly two daughters, we extend the matrix C , by doubling the number of rows (i.e. mothers), stacking two identical rectangular matrices on top of each other:

$$C_{2m \times d} = \begin{bmatrix} \hat{C}_{m \times d} \\ \hat{C}_{m \times d} \end{bmatrix} \quad (6)$$

where

$$\hat{C}_{m \times d} = \begin{bmatrix} L(1, 1) & L(1, 2) & \dots & L(1, d) \\ L(2, 1) & L(2, 2) & \dots & L(2, d) \\ \vdots & \vdots & \vdots & \vdots \\ L(m, 1) & L(m, 2) & \dots & L(m, d) \end{bmatrix} \quad (7)$$

To solve the formulated problem, we use a modified Jonker-Volgenant algorithm without initialization [26], implemented in [28]. This algorithm also solves a generalization of the classic assignment problem, where the cost matrix (C) is rectangular. If C has more rows than columns, then not every

row needs to be assigned to a column, and vice versa. In case of an odd number of daughters when $d > 2m$, i.e., a new cell that was not present at frame t appears in frame $t + 1$, this cell is left unassigned. On the contrary, when $d < 2m$, i.e., one of the daughters from frame $t + 1$ disappears, the mother is only assigned one daughter. The pseudocode of the proposed cell tracking strategy for two consecutive frames is shown as Algorithm 1.

Algorithm 1: The proposed two-stage assignment strategy

Data: Segmentation masks, Activity maps

Result: Cell pairs

for $t \leftarrow 0$ **to** $N - 1$ **do**

$Mothers \leftarrow$ [all cells in t];

sort ($Mothers$, ascending Activity);

$Daughters \leftarrow$ [all cells in $t + 1$];

$Pairs \leftarrow$ [];

for every $cell_i$ **in** $Mothers$ **do**

$\mathcal{L} \leftarrow$ [];

for every $cell_j$ **in** $Daughters$ **do**

| $\mathcal{L}.append(L_{i,j})$

end

if $area(cell_i) > area(cell_{\text{argmin}(\mathcal{L})})$ **then**

| remove $cell_{\text{argmin}(\mathcal{L})}$ from $Daughters$;

| remove $cell_i$ from $Mothers$;

| $Pairs.append([cell_i, cell_{\text{argmin}(\mathcal{L})})$

end

end

$C \leftarrow L(Mothers, Daughters)$;

$Pairs.append(linear_sum_assignment(C))$;

end

IV. RESULTS

A. Ground truth generation

To create a ground truth, we applied the proposed and a baseline approach (see below) to the segmented highest time-resolution dataset. In doing so, we carefully checked manually, and refined if needed, the obtained lineage. The original image sequences of the *C. glutamicum* and *E. coli* consist of 244 and 99 frames, respectively. In order to evaluate our algorithm for different frame rates, i.e. 2, 4, 6, 8, 10, and 12 minutes for *C. glutamicum* and 5, 10, 15 minutes for *E. coli*, we down-sample our original datasets, respectively.

Additionally, we hope that the conducted frame rate sensitivity analysis of the algorithm for *C. glutamicum* and *E. coli* will provide insights to the biotechnologists about the choice of the frame rate for their cell cultivation experiments, offering a trade-off between tracking accuracy and microscopy settings.

B. Comparison to a baseline approach

We use the tracking accuracy (TRA) from the cell tracking challenge [10] to evaluate the performance of the proposed algorithm. The TRA score is based on the acyclic-oriented graph matching measure [29], which penalizes the number of transformations needed to transform the predicted tracking graph into the ground truth tracking graph. The measure penalizes errors of the detection (false positives, false negatives) and errors concerning merged cells and tracking (missing links, wrong links, and links with wrong semantics). Since our goal is to evaluate the tracking correctness only, we provide the ground truth segmentation for both baseline and the proposed approach and do not expect any detection-related errors.

As baseline algorithm, we use a graph-based cell tracking algorithm [16], being ranked in the top three for the majority of the datasets of the cell tracking challenge. The baseline algorithm offers segmentation refinement, such as untangling and false negative correction. Since, in our case, the tracking was performed on the ground truth segmentation with no need for refinement, we use two variants of the baseline approach: the algorithm with default parameter settings (`postprocessing_key=None`), and without the segmentation refinement step (`postprocessing_key='nd_ns+1'`). In case of *E. coli* dataset evaluation, both settings lead to the same result, so we only report the value at default settings (Fig. 5).

The high TRA values in the obtained plots are explained by the fact that, the TRA measure's penalty factor (p) for the wrong detections: splitting operations ($p=5$), false negative vertices ($p=10$), false positive vertices ($p=1$) is considerably higher, than for the wrong associations: redundant edges to be deleted ($p=1$), edges to be added ($p=1.5$) and edges with wrong semantics ($p=1$). Nevertheless, we use the TRA measure since it is known in the community, standardized and provides an unbiased comparison of the methods.

As shown in Fig. 5, the proposed method outperforms the baseline method when applied to a *C. glutamicum* dataset and is on par with the baseline approach applied to the

E. coli dataset. The cross-correlation nature of the baseline approach and relatively simple (no snapping, the angle of daughters is preserved) division behavior of *E. coli*, explains the slightly better results of the method, whereas the proposed method handles the complex V-snapping division behavior of *C. glutamicum* better. Moreover, in case of the *E. coli* dataset, the septum formation as a part of the division process may not be captured in the phase contrast images. Therefore, the cell splitting events are sometimes not highlighted on the activity map. To overcome this, the fluorescence may be used to feature the septum formation [30].

V. CONCLUSION

We proposed a novel tracking-free mapping of active cells — the activity map. The activity map is useful as a standalone metric of cell activity, a tool to be used in tracking annotation software to attract the user's attention to the "changing" cells, or a building block for cell tracking. Additionally, we introduced a feature-free tracking approach that utilizes the activity map. The proposed tracking method consists of two steps: a prioritized single-cell assignment strategy of growing (non-splitting) cells and a combinatorial mother-daughter assignment of the dividing cells. We evaluated the proposed algorithm on datasets representing two important biotechnologically relevant rod-shaped microorganisms: *C. glutamicum*, with peculiar V-snapping division behavior, and *E. coli*, which divides uniformly by linear elongation. The numerical experiments show that the proposed tracking approach outperforms the baseline approach in *C. glutamicum* tracking and is on par with the baseline approach in *E. coli* tracking. Additionally, we evaluate the algorithm's performance on datasets with different frame rates. We hope that the reported tracking quality metrics can provide insights to the biotechnologists and help them to choose the proper frame rate for their cultivation experiments.

Our source code is available on GitHub <https://github.com/kruzaeva/activity-cell-tracking>

REFERENCES

- [1] Alexander Manuel Grünberger, *Single-cell analysis of microbial production strains in microfluidic bioreactors*, Schriften des Forschungszentrums Jülich Reihe Schlüsseltechnologien / Key Technologies. Forschungszentrum Jülich, 2015.
- [2] Axel Theorell, Johannes Seiffarth, Alexander Grünberger, and Katharina Nöh, "When a single lineage is not enough: Uncertainty-aware tracking for spatio-temporal live-cell image analysis," *Bioinformatics*, vol. 35, no. 7, pp. 1221–1228, sep 2018.
- [3] Mirela T. Cazzolato, Agma J. M. Traina, and Klemens Böhm, "Efficient and reliable estimation of cell positions," in *Proceedings of the 27th ACM International Conference on Information and Knowledge Management*. oct 2018, ACM.
- [4] M. Maska, O. Danek, S. Garasa, A. Rouzaut, A. Munoz-Barrutia, and C. Ortiz de Solorzano, "Segmentation and shape tracking of whole fluorescent cells based on the chan-veye model," *IEEE Transactions on Medical Imaging*, vol. 32, no. 6, pp. 995–1006, jun 2013.
- [5] O. Dzyubachyk, W.A. van Cappellen, J. Essers, W.J. Niessen, and E. Meijering, "Advanced level-set-based cell tracking in time-lapse fluorescence microscopy," *IEEE Transactions on Medical Imaging*, vol. 29, no. 3, pp. 852–867, mar 2010.
- [6] Assaf Arbelle, Jose Reyes, Jia-Yun Chen, Galit Lahav, and Tammy Riklin Raviv, "A probabilistic approach to joint cell tracking and segmentation in high-throughput microscopy videos," *Medical Image Analysis*, vol. 47, pp. 140–152, jul 2018.

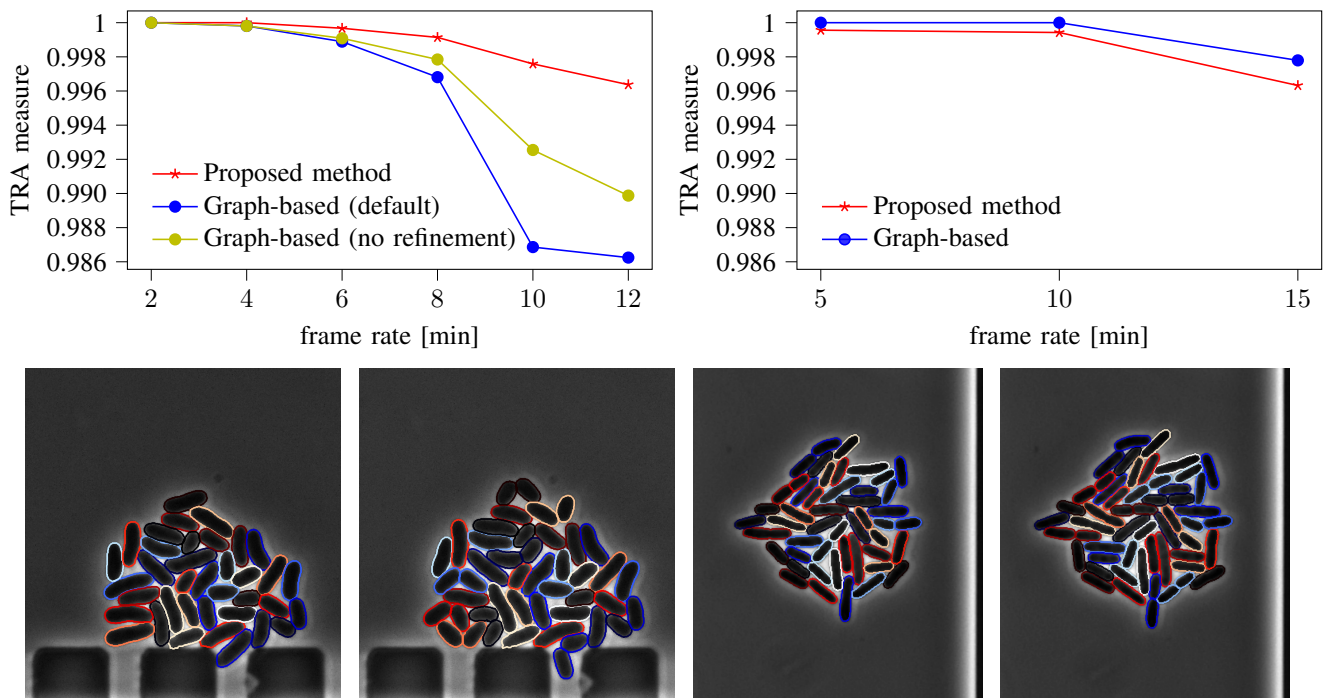


Fig. 5. Top row: A quantitative comparison of the proposed method vs. the baseline approach for different frame rates and two different microorganisms: *C. glutamicum* (left) and *E. coli* (right). The bottom row illustrates the tracking results of the proposed method for two consecutive frames of *C. glutamicum* (12 min) and *E. coli* (15 min), from left to right, respectively. Here, the color of the cell contour in t is preserved for the same cell in $t + 1$, as well as for both daughter cells, in the case of the cell's division.

- [7] Kevin J. Cutler, Carsen Stringer, Paul A. Wiggins, and Joseph D. Mougous, "Omnipose: a high-precision morphology-independent solution for bacterial cell segmentation," *bioRxiv*, nov 2021.
- [8] Carsen Stringer, Tim Wang, Michalis Michaelos, and Marius Pachitariu, "Cellpose: a generalist algorithm for cellular segmentation," *Nature Methods*, vol. 18, no. 1, pp. 100–106, dec 2020.
- [9] Karina Ruzaeva, Katharina Nöh, and Benjamin Berkels, "A hybrid multi-object segmentation framework with model-based b-splines for microbial single cell analysis," in *2022 IEEE 19th International Symposium on Biomedical Imaging (ISBI)*, mar 2022, IEEE.
- [10] Vladimír Ulman et al., "An objective comparison of cell-tracking algorithms," *Nature Methods*, vol. 14, no. 12, pp. 1141–1152, oct 2017.
- [11] Andreas P. Cuny, Aaron Ponti, Tomas Kündig, Fabian Rudolf, and Jörg Stelling, "Cell region fingerprints enable highly precise single-cell tracking and lineage reconstruction," *bioRxiv*, oct 2021.
- [12] Jean-Yves Tinevez et al., "TrackMate: An open and extensible platform for single-particle tracking," *Methods*, vol. 115, pp. 80–90, feb 2017.
- [13] Diane H. Theriault, Matthew L. Walker, Joyce Y. Wong, and Margrit Betke, "Cell morphology classification and clutter mitigation in phase-contrast microscopy images using machine learning," *Machine Vision and Applications*, vol. 23, no. 4, pp. 659–673, jun 2011.
- [14] Athanasios D. Balomenos, Panagiotis Tsakanikas, and Elias S. Manolakos, "Tracking single-cells in overcrowded bacterial colonies," in *2015 37th Annual International Conference of the IEEE Engineering in Medicine and Biology Society (EMBC)*, aug 2015, IEEE.
- [15] Sorena Sarmadi et al., "Stochastic neural networks for automatic cell tracking in microscopy image sequences of bacterial colonies," *Mathematical and Computational Applications*, vol. 27, no. 2, pp. 22, mar 2022.
- [16] Katharina Löffler, Tim Scherr, and Ralf Mikut, "A graph-based cell tracking algorithm with few manually tunable parameters and automated segmentation error correction," *PLOS ONE*, vol. 16, no. 9, pp. e0249257, sep 2021.
- [17] Klas E. G. Magnusson, Joakim Jalden, Penney M. Gilbert, and Helen M. Blau, "Global linking of cell tracks using the viterbi algorithm," *IEEE Transactions on Medical Imaging*, vol. 34, no. 4, pp. 911–929, apr 2015.
- [18] Simone Schito et al., "Communities of niche-optimized strains (CoNos) – design and creation of stable, genome-reduced co-cultures," *Metabolic Engineering*, vol. 73, pp. 91–103, sep 2022.
- [19] Katharina Löffler and Ralf Mikut, "Embedtrack – simultaneous cell segmentation and tracking through learning offsets and clustering bandwidths," 2022.
- [20] Jean-Baptiste Lugagne, Haonan Lin, and Mary J. Dunlop, "DeLTA: Automated cell segmentation, tracking, and lineage reconstruction using deep learning," *PLOS Computational Biology*, vol. 16, no. 4, pp. e1007673, apr 2020.
- [21] Sang Yup Lee, Ed., *Systems Biology and Biotechnology of Escherichia coli*, Springer Dordrecht, 2009.
- [22] Eugen Kaganovitch, Xenia Steurer, Deniz Dogan, Christopher Probst, Wolfgang Wiechert, and Dietrich Kohlheyer, "Microbial single-cell analysis in picoliter-sized batch cultivation chambers," *New Biotechnology*, vol. 47, pp. 50–59, dec 2018.
- [23] Lothar Eggeling and Michael Bott, Eds., *Handbook of Corynebacterium glutamicum*, CRC Press, mar 2005.
- [24] Xiaoxue Zhou et al., "Sequential assembly of the septal cell envelope prior to v snapping in *Corynebacterium glutamicum*," *Nature Chemical Biology*, vol. 15, no. 9, pp. 221–231, sep 2019.
- [25] Noga Mosheiff et al., "Inheritance of cell-cycle duration in the presence of periodic forcing," *Phys. Rev. X*, vol. 8, pp. 021035, May 2018.
- [26] David F. Crouse, "On implementing 2d rectangular assignment algorithms," *IEEE Transactions on Aerospace and Electronic Systems*, vol. 52, no. 4, pp. 1679–1696, aug 2016.
- [27] Rainer Burkard, Mauro Dell'Amico, and Silvano Martello, *Assignment Problems*, Society for Industrial and Applied Mathematics, 2012.
- [28] Pauli Virtanen et al., "SciPy 1.0: Fundamental Algorithms for Scientific Computing in Python," *Nature Methods*, vol. 17, pp. 261–272, 2020.
- [29] Pavel Matula, Martin Maška, Dmitry V. Sorokin, Petr Matula, Carlos Ortiz de Solórzano, and Michal Kozubek, "Cell tracking accuracy measurement based on comparison of acyclic oriented graphs," *PLOS ONE*, vol. 10, no. 12, pp. e0144959, dec 2015.
- [30] Qin Sun and William Margolin, "Ftsz dynamics during the division cycle of live escherichia coli cells.," *Journal of Bacteriology*, vol. 180, no. 8, pp. 2050–2056, apr 1998.